Intense winter surface melt on an Antarctic ice shelf

Munneke, P. Kuipers; Luckman, A. J.; Bevan, S. L.; Smeets, C. J. P. P.; Gilbert, E.; Van Den Broeke, M. R.; Wang, W.; Zender, C.; Hubbard, B.; Ashmore, D.; Orr, A.; King, J. C.; Kulessa, B.

Published in:
Geophysical Research Letters

DOI:
10.1029/2018GL077899

Publication date:
2018

Citation for published version (APA):
Munneke, P. K., Luckman, A. J., Bevan, S. L., Smeets, C. J. P. P., Gilbert, E., Van Den Broeke, M. R., Wang, W., Zender, C., Hubbard, B., Ashmore, D., Orr, A., King, J. C., & Kulessa, B. (2018). Intense winter surface melt on an Antarctic ice shelf. *Geophysical Research Letters*, *45*(15), 7615-7623. https://doi.org/10.1029/2018GL077899

Geophysical Research Letters

RESEARCH LETTER
10.1029/2018GL077899

Key Points:
- Wintertime surface melt occurs frequently in the Antarctic Peninsula
- Winter melt heats the firn to a depth of about 3 m, retarding or reversing winter cooling
- Increased greenhouse gas concentrations could increase the occurrence of winter surface melt

Correspondence to:
P. Kuipers Munneke,
p.kuipersmunneke@uu.nl

Citation:
Kuipers Munneke, P., Luckman, A. J., Bevan, S. L., Smeets, C. J. P. P., Gilbert, E., van den Broeke, M. R., et al. (2018). Intense winter surface melt on an Antarctic ice shelf. *Geophysical Research Letters*, *45*. https://doi.org/10.1029/2018GL077899

Received 12 MAR 2018
Accepted 21 APR 2018
Accepted article online 2 MAY 2018

Intense Winter Surface Melt on an Antarctic Ice Shelf

P. Kuipers Munneke[1], A. J. Luckman[2], S. L. Bevan[2], C. J. P. P. Smeets[1], E. Gilbert[3,4], M. R. van den Broeke[1], W. Wang[5], C. Zender[5], B. Hubbard[6], D. Ashmore[7], A. Orr[3], J. C. King[3], and B. Kulessa[2]

[1]Institute for Marine and Atmospheric research Utrecht, Utrecht University, Utrecht, Netherlands, [2]Department of Geography, Swansea University, Swansea, UK, [3]British Antarctic Survey, Natural Environment Research Council, Cambridge, UK, [4]School of Environmental Sciences, University of East Anglia, Norwich, UK, [5]Department of Earth System Science, University of California, Irvine, CA, USA, [6]Centre for Glaciology, Department of Geography and Earth Sciences, Aberystwyth University, Aberystwyth, UK, [7]School of Environmental Sciences, University of Liverpool, Liverpool, UK

Abstract The occurrence of surface melt in Antarctica has hitherto been associated with the austral summer season, when the dominant source of melt energy is provided by solar radiation. We use in situ and satellite observations from a previously unsurveyed region to show that events of intense surface melt on Larsen C Ice Shelf occur frequently throughout the dark Antarctic winter, with peak intensities sometimes exceeding summertime values. A regional atmospheric model confirms that in the absence of solar radiation, these multiday melt events are driven by outbreaks of warm and dry föhn wind descending down the leeside of the Antarctic Peninsula mountain range, resulting in downward turbulent fluxes of sensible heat that drive sustained surface melt fluxes in excess of 200 W/m^2. From 2015 to 2017 (including the extreme melt winter of 2016), ~23% of the annual melt flux was produced in winter, and spaceborne observations of surface melt since 2000 show that wintertime melt is widespread in some years. Winter melt heats the firn layer to the melting point up to a depth of ~3 m, thereby facilitating the formation of impenetrable ice layers and retarding or reversing autumn and winter cooling of the firn. While the absence of a trend in winter melt is consistent with insignificant changes in the observed Southern Hemisphere atmospheric circulation during winter, we anticipate an increase in winter melt as a response to increasing greenhouse gas concentration.

Plain Language Summary Around the coast of Antarctica, it gets warm enough in summer for snow to start melting, and the sun provides most of the energy for that melt. Almost all meltwater refreezes in the snowpack, but especially on floating glaciers in Antarctica, it has been observed that meltwater forms large ponds. The pressure exerted by these ponds may have led to ice shelves collapsing into numerous icebergs in recent decades. It is therefore important to understand how much meltwater is formed. To find out, we installed an automatic weather station on a glacier in Cabinet Inlet, in the Antarctic Peninsula in 2014. The station recorded temperatures well above the melting point even in winter. The occurrence of winter melt is confirmed by satellite images and by thermometers buried in the snow, which measured a warming of the snow even at 3 m depth. Between 2014 and 2017, about 23% of all melt in Cabinet Inlet occurred in winter. Winter melt is due to warm winds that descend from the mountains, known as föhn. We have not seen the amount of winter melt increasing since 2000. However, we expect winter melt to happen more frequently if greenhouse gas continues to accumulate in the atmosphere.

1. Surface Melt in Antarctica

Current mass loss of the Antarctic Ice Sheet is made up almost entirely of ice shelf basal melting and iceberg calving (Depoorter et al., 2013). Although supraglacial and englacial runoff has been widely observed, especially in regions of low albedo such as blue ice and bare rock (Bell et al., 2017; Kingslake et al., 2017; Lenaerts et al., 2016), models suggest that only a small fraction (<1%) of the ~115 Gt (1 Gt = 10^{12} kg) of surface meltwater produced annually (Trusel et al., 2013; Van Wessem et al., 2017) runs off directly into the ocean. Instead, it is refrozen within underlying snow and firn layers (Kuipers Munneke, Picard, et al., 2012). The indirect impact of meltwater is profound, however, as an important role for meltwater-induced fracturing is implicated in the collapse of coastal ice shelves (Banwell et al., 2013; Scambos et al., 2000). Observed collapse following

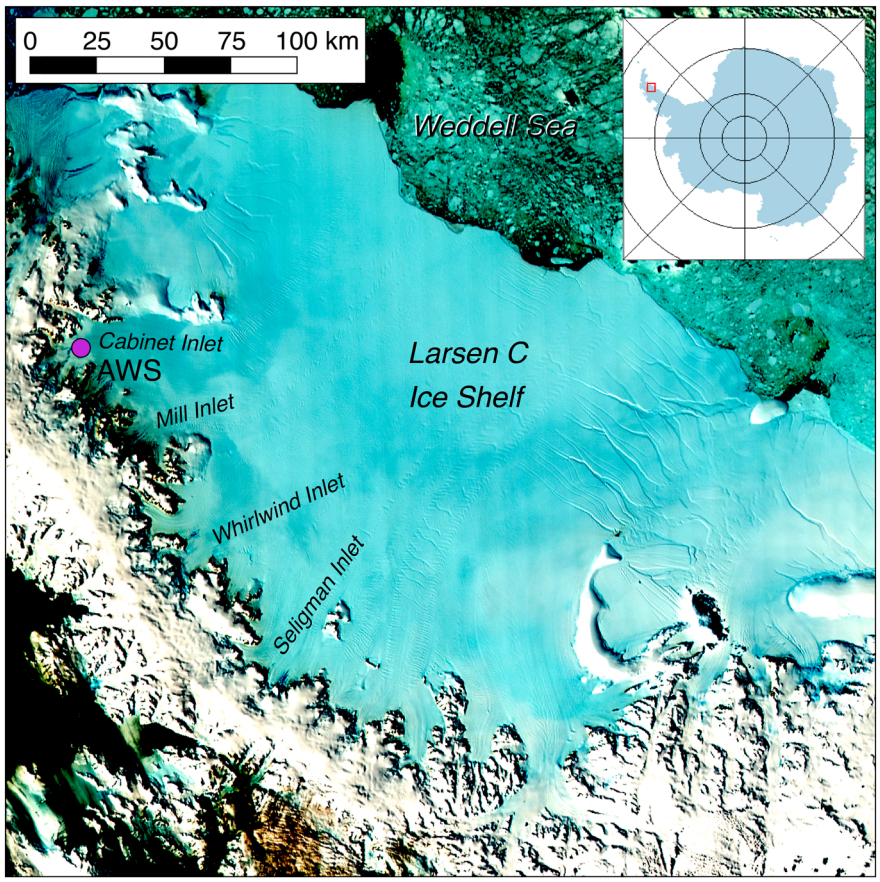

Figure 1. False-color Moderate Resolution Imaging Spectroradiometer image of Larsen C Ice Shelf in 2016. The magenta circle indicates the location of the automatic weather station (AWS) in Cabinet Inlet.

atmospheric warming (Abram et al., 2013) led to a manifold acceleration of grounded-ice flow (De Angelis & Skvarça, 2003; Rott et al., 2011), explaining part of the increased dynamic ice loss witnessed in the Antarctic Peninsula in recent decades (Harig & Simons, 2015). Further loss of ice shelves may induce rapid retreat by mechanical failure of grounded-ice cliffs (Bassis & Walker, 2012; DeConto & Pollard, 2016). Ice shelves may become more vulnerable to breakup due to sustained high rates of surface meltwater refreezing, which warms and softens the ice englacially (Hubbard et al., 2016; Phillips et al., 2010) and ultimately removes the layer of snow and firn (Kuipers Munneke et al., 2014).

Model- and satellite-derived surface melt rates range from less than 20 mm w.e./year on ice shelves in Dronning Maud Land and the Amundsen Sea sector to ~250 mm w.e./year on average over Larsen C Ice Shelf, with certain sectors of Larsen C peaking at 400 mm w.e./year (Trusel et al., 2013). In summer, the bulk of the energy for snowmelt in Antarctica is provided by solar radiation, which is only partly offset by turbulent fluxes of sensible and latent heat directed away from the surface (Van den Broeke et al., 2005). In winter, the sensible heat flux is directed toward the surface, to compensate for the absence of solar radiation and consequent surface cooling. Winter temperatures above the melting point of snow have been reported in the Antarctic Peninsula (e.g., Cape et al., 2015; Kuipers Munneke, Picard, et al., 2012; Leeson et al., 2017), in conjunction with warm and dry downslope winds known as föhn. In particular, Leeson et al. (2017) discuss that strong, likely föhn-related autumnal melting led to high surface melt fluxes 2 years before collapse of the Larsen B Ice Shelf in 2002. Föhn-induced melt is also observed in spring (King et al., 2017). Overall, however, the inventory of winter surface melt has been very sparse. Here we report peak annual melt fluxes in the austral winter, derived from measurements from an automatic weather station (AWS) located in Cabinet Inlet, a climatologically unsurveyed area of Larsen C Ice Shelf in the Antarctic Peninsula (Figure 1 and Appendix A), and for the first time discuss the occurrence, significance, context, and impact of wintertime surface melt in Antarctica.

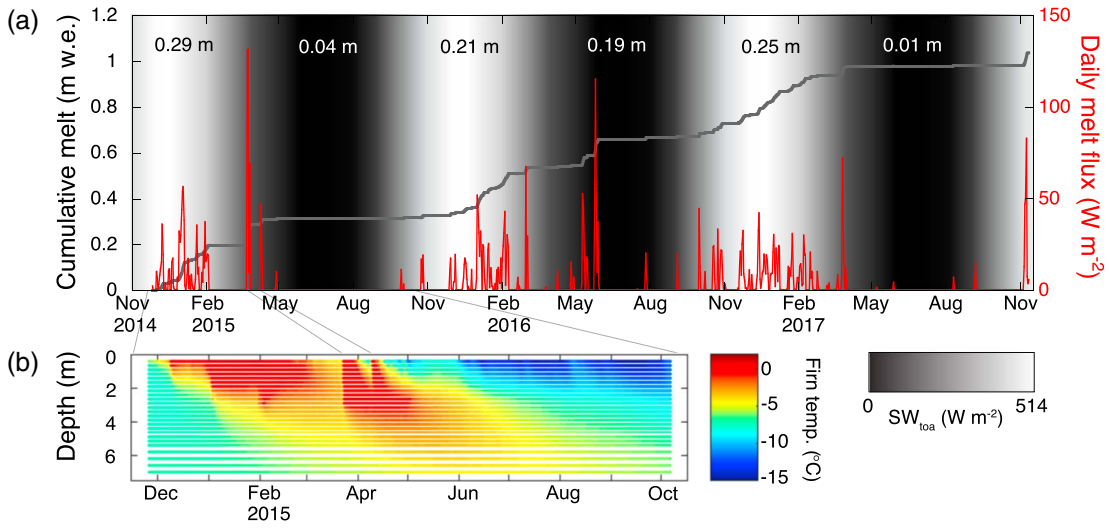

Figure 2. (a) Daily mean melt flux (W/m^2, red) and cumulative melt (m w.e., gray) for November 2014 to November 2017, computed from automatic weather station observations. Background gradient shows daily mean top-of-atmosphere incoming solar radiation, SW_{toa}: black is 0, white is 514 W/m^2. Text labels in the top of the panel denote cumulative melt (m w.e.) for austral summer (1 November to 31 March) and winter (1 April to 31 October) seasons. (b) Thermistor string observations of firn temperature (°C) as a function of depth (m), in 2015.

2. In Situ Observation of Winter Melt

Almost 3 years of AWS observations (25 November 2014 to 13 November 2017) were used to drive a model of the snow surface energy budget (Appendix B; Kuipers Munneke, van den Broeke, et al., 2012). It simulates a cumulative melt of 1,040 mm w.e. in Cabinet Inlet (Figure 2), equating to a melt rate of 350 mm w.e./year. We find that only 77% of the cumulative melt (800 mm w.e.) occurs in the austral summer season, which we define here to last from 1 November to 31 March. This summer melt mostly occurs in prolonged episodes of days to weeks, with peak daily melt fluxes of 40–60 W/m^2. Melt energy in these conditions is supplied by absorbed solar radiation (Kuipers Munneke, van den Broeke, et al., 2012). Thus, 23% of the surface melt in the period under consideration (240 mm w.e.) is generated in the winter season, here defined from 1 April to 31 October. Most of the observed wintertime melt occurred in the austral winter of 2016 (190 mm w.e.), with smaller fractions in 2015 (50 mm w.e.) and 2017 (10 mm w.e.). Over the three years recorded, wintertime surface melt took place in all months except July. In contrast to summer melt, the winter melt episodes are usually shorter (at most a few days) and more intense, with daily mean melt fluxes ranging from 25 to over 120 W/m^2 (equating to a melt rate of 6–31 mm w.e./day).

The strongest wintertime melt episode in the record occurred on 25–30 May 2016 (Figure 3) and featured observed melt fluxes that greatly exceeded those seen during summer. A combination of high observed wind speed (5–18 m/s) and warm air (5–13°C at 2 m above the surface) resulted in a large turbulent flux of sensible heat downward to the surface. Negative fluxes of longwave radiation (longwave cooling and under clear skies) and latent heat (sublimation) offset some of this sensible heat flux. Still, the resulting melt flux is dominated by sensible heat transfer, which frequently reaches up to 200 W/m^2 with sustained extremes of >300 W/m^2 lasting for up to 30 min (the recording resolution of the AWS data). In total, 71 mm of meltwater was produced as a consequence of this föhn event. During melt, the strong winds advect air that is dried by adiabatic warming, with relative humidity between 35% and 65%.

3. Cause and Consequence

The combination of strong wind, high temperature, and low relative humidity is common to all wintertime melt events. These are fingerprints for föhn winds that sometimes occur over the Antarctic Peninsula mountain range. Such föhn winds are caused by flow across a topographic barrier, whereby the downslope winds on the leeward side are heated adiabatically (Kuipers Munneke, van den Broeke, et al., 2012; Luckman et al., 2014). Additional heating can occur due to the drawdown of potentially warm and dry air from aloft when the flow is blocked at lower levels on the windward side and due to entrainment of potentially warm and dry air from upper levels into the flow over the mountains (Orr et al., 2008). The vertical cross section (Figure 3d) over

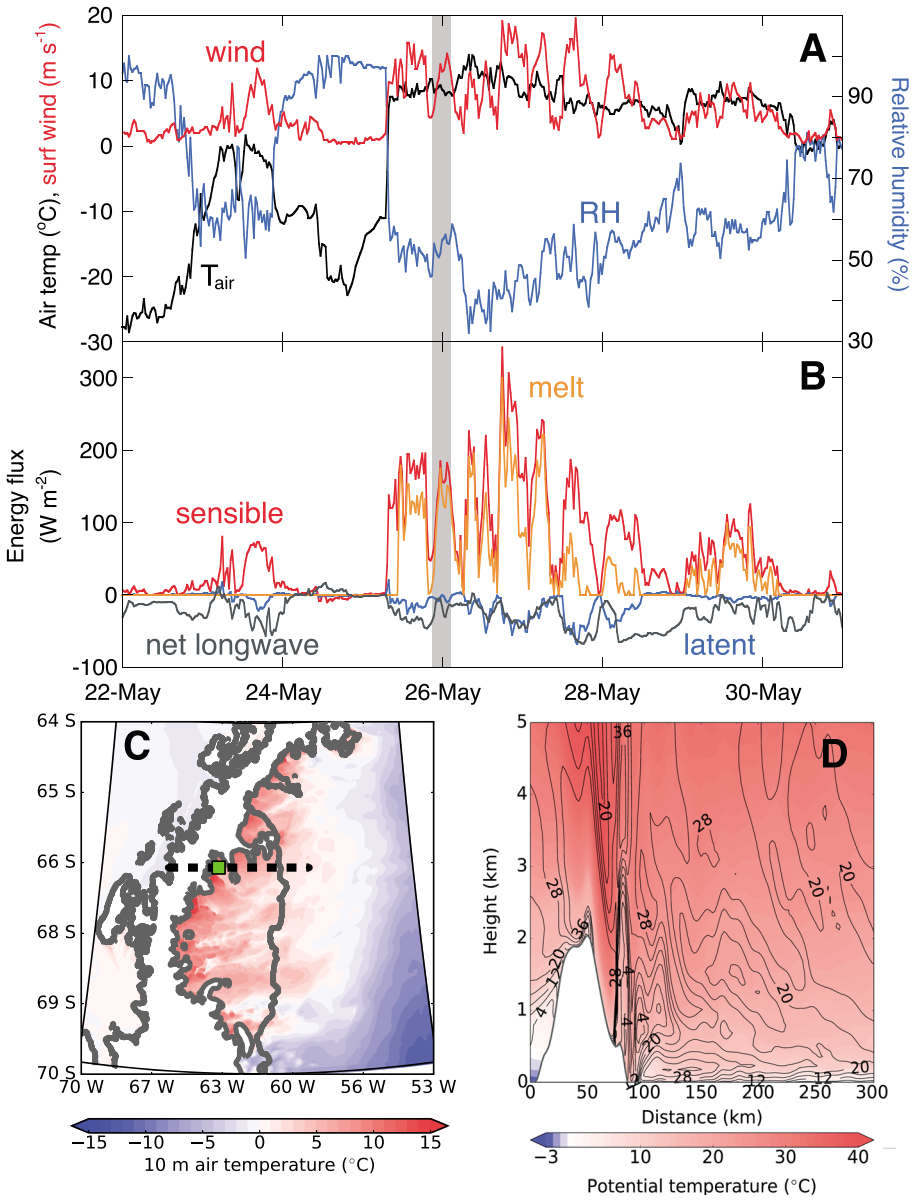

Figure 3. Hourly values of observed meteorological conditions and surface energy balance in Cabinet Inlet, 22–31 May 2016. (a) Air temperature (at 2 m above the surface, °C, black), wind speed (at 10 m above the surface, m/s, red), relative humidity (at 2 m above the surface, %, blue). The vertical gray bar indicates the time of the model snapshots in panels (c) and (d). (b) Net longwave radiation (gray), turbulent fluxes of sensible (red) and latent (blue) heat, and melt flux (orange). All fluxes in W/m^2. (c) Map showing modeled temperature (in °C) at 10 m above sea level over Larsen C, on 26 May 2016 at 00:00 UTC. The dashed line indicates the location of the transect shown in panel (d), and the green square shows the location of the Cabinet Inlet automatic weather station. (d) Modeled vertical cross section through the Antarctic Peninsula mountains into Cabinet Inlet on 26 May 2016 at 00:00 UTC. Filled color contours show potential temperature (in °C), and black open contours show wind speed (in m/s).

the Antarctic mountain range through Cabinet Inlet from a high-resolution regional atmospheric model (the UK MetOffice Unified Model, see Appendix C) confirms the occurrence of föhn during 25–30 May 2016, with moist air rising on the windward side of the mountains and relatively dry, adiabatically warmed air descending on its leeside. In the lee of the mountains, a hydraulic jump is apparent in the vertical wind component (at about 70 km on the horizontal axis in Figure 3d), characteristic of föhn (Elvidge & Renfrew, 2016).

The regional atmospheric model further shows that during this event, temperature at 10 m above the surface was above the melting point for most of the ice shelf, indicative of widespread surface melt not restricted

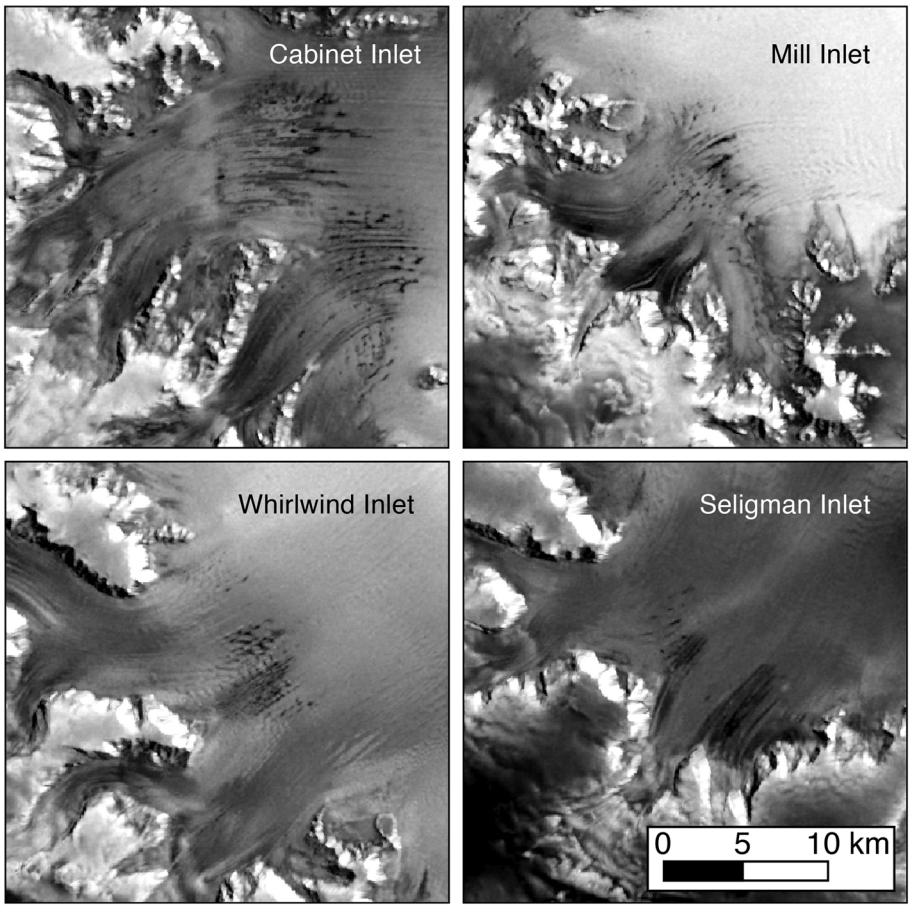

Figure 4. Sentinel 1A C-band synthetic aperture radar imagery from locations near the grounding line of Larsen C Ice Shelf. Elongated black features on the ice shelf indicate meltwater lakes and ponds. See Figure 1 for locations of the inlets.

to Cabinet Inlet (see Figure 3c). A collection of synchronous Sentinel-1A synthetic aperture radar images of a part of Larsen C Ice Shelf (Figure 4), taken near the end of the May 2016 föhn event, confirms that surface melt was occurring beyond Cabinet Inlet. It shows extensive snow melt across the northwestern and western inlets of the shelf (apparent in the satellite images as dark-hued areas), along with a large number of meltwater lakes collected in local depressions of the ice shelf (shown as black elongated features in the images of Figure 4). The elongated depressions express channels in the basal topography, possibly arising from buoyant basal meltwater generated at the grounding line (Sergienko, 2013) or from the grounded ice being extruded over a strongly undulating grounding line (Gladish et al., 2012).

Wintertime meltwater is able to percolate deeply into the snowpack, bringing snow temperatures to the melting point up to a depth of about 3 m (Figure 2b) when latent heat is released as the meltwater refreezes. Observations from thermistor-instrumented boreholes (Appendix D) suggest that effective pathways for this major source of latent energy are available year-round, as even during winter melt, the warming of near-surface layers is almost instantaneous (e.g., in two episodes of melt during end of March and April 2015, apparent in Figure 2b, percolation to 3 m depth occurred in about 12 hr). As a consequence, winter melt warms the snowpack, allowing for an earlier start of the main melt season in spring and summer and heating of the deeper ice layers. Also, it forms relatively impermeable infiltration ice (Hubbard et al., 2016) that can act as a runoff surface for meltwater (Bell et al., 2017).

4. Past, Present, and Future Winter Melt

To put the occurrence of wintertime surface melt into a longer-term perspective, we use satellite-borne Quik Scatterometer (QuikSCAT) (2000–2009) and Advanced Scatterometer (ASCAT) (2009–2016) scatterometer

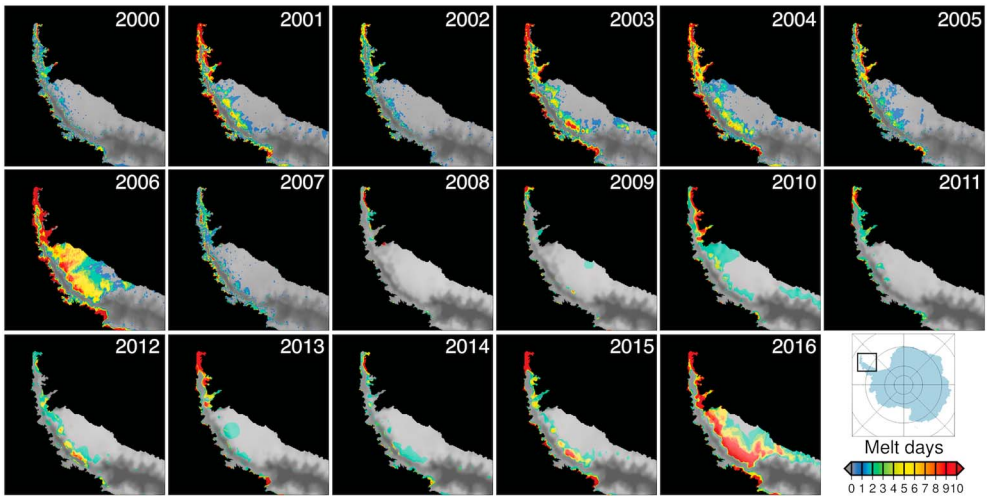

Figure 5. Maps over the Antarctic Peninsula showing annual number of melt days per winter (1 April to 31 October) between 2000 and 2016, observed by QuikSCAT (2000–2009) and ASCAT (2010–2016).

sensors to estimate the number of melt days over the Antarctic Peninsula for each winter season (Figure 5 and Appendix E). Radar scatterometry is an active remote sensing technique that is sensitive to the presence of liquid water in snow or firn. While the presence of liquid water does not necessarily imply the occurrence of surface melt, the two are highly correlated (Van den Broeke et al., 2010). In some years, little or no meltwater is present during winter, whereas in other years, the number of days with liquid water present on Larsen C approaches 10. In all years, we see enhanced melt over the Larsen C Ice Shelf near the base of the eastern slopes of the Antarctic Peninsula mountain range, which is consistent with föhn-driven warming (Luckman et al., 2014). Near the calving front of Larsen C, wintertime melt occurred in the extreme melt winter of 2006 and to a lesser extent in 2016. These stand out in our records as the most intense winter melt seasons since 2000.

No trend in the occurrence of winter melt over Larsen C is evident over the 17-year record of satellite scatterometry, which implies that there have been no contemporaneous changes in the frequency or duration of westerly föhn events in winter over the Antarctic Peninsula. This is consistent with the absence of any statistically significant winter trends in the Southern Annular Mode (SAM), which is the principal mode of Southern Hemisphere extratropical climate variability, during the scattermometry period considered or even since 1958 (Marshall, 2003). By contrast, the SAM has shifted toward a more positive phase in summer in recent decades (Marshall, 2003), resulting in increased westerly flow over the Antarctic Peninsula and associated föhn events (Marshall et al., 2006; Orr et al., 2008). These led to anomalous warming and melt due to föhn (Cape et al., 2015). As the winter SAM is projected to trend toward its positive phase during the 21st century because of increased greenhouse gas concentrations (Simpkins & Karpechko, 2012), we can thus expect an enhancement of winter melt in this century, from atmospheric circulation changes alone. The magnitude of this effect increases with the atmospheric concentration of greenhouse gases (Zheng et al., 2013).

Ice shelf collapse by hydrofracturing is implicated in future scenarios of rapid Antarctic ice discharge and sea level rise (DeConto & Pollard, 2016). For these processes to be understood and predicted, a reliable estimate of future surface melt and its impact on the state of the firn layer on ice shelves is required. Such estimates can only be achieved if subtle processes like the formation of impermeable ice layers, winter warming, and densification of firn, due to meltwater percolation, ponding, and refreezing, are appropriately taken into account.

Appendix A: Automatic Weather Station

An AWS was installed in Cabinet Inlet (66°24.1′S, 63°22.3′W) in November 2014. Data were recorded at half-hourly resolution. Instrument height was monitored and usually between 1.7 and 2.4 m above the surface. Reported quantities are at a nominal levels of 2 m for temperature and humidity and 10 m for wind speed. Shortwave radiation was tilt corrected using a Moderate Resolution Imaging Spectroradiometer

satellite-guided procedure (Wang et al., 2016). Air temperature observations were unventilated, leading to overestimation during calm, sunny days. A correction function was derived from concurrent thermocouple observations during November 2014 through January 2015. Observations of relative humidity were corrected for solar heating of the housing of the humidity sensor and for hysteresis effects due to a long response time of the sensor.

Appendix B: Surface Energy Balance Model

The surface energy balance was computed using a model that includes a multilayer snowpack. The model forces the energy budget to close by iterating to a surface temperature for which all the terms balance (Kuipers Munneke, Picard, et al., 2012). If that temperature is above the freezing point, all excess energy is used for melting, and the surface temperature (and associated outgoing longwave radiation) is set to the melting point. The model is evaluated by comparing computed surface temperature with observed values (computed from the outgoing longwave radiation with the Stefan-Boltzmann law). The difference between these is 0.21 K on average (RMS = 1.85 K; RMS = root-mean-square). Further, the timing of melt is corroborated with surface height lowering observed by a sonic height ranger attached to the AWS mast and by observations of outgoing longwave radiation indicating the surface temperature to be at the melting point.

Appendix C: Regional Atmospheric Model

Version 10.4 of the UK Met Office Unified Model (Orr et al., 2014) is used to downscale operational analysis data to a horizontal grid spacing of 1.5 km, a resolution sufficient to represent föhn over the Antarctic Peninsula reasonably well (Elvidge et al., 2014). The 1.5 km inner domain, encompassing the Larsen C Ice Shelf and the adjacent region of the Antarctic Peninsula (see Figure 3C) is nested within a 4 km outer domain that includes the entire Antarctic Peninsula. Boundary and surface conditions for the outer domain are provided by a global, 25 km version of the Unified Model, which is driven by Met Office operational data. Only results from the 1.5 km domain are examined here.

Appendix D: Borehole Thermistor Strings

Firn temperatures were measured using a string of NTC thermistors in a Wheatstone half-bridge and recorded every 30 min using a Campbell Scientific data logger. Resistances were converted to temperatures using a Steinhart-Hart equation (Steinhart & Hart, 1968) and the manufacturer calibration data. A second calibration was performed by using a well-mixed distilled water/ice bath, assumed to be 0°C, to derive the zero offset for each thermistor. After-correction sensors gave an RMS error of ±0.03°C in an identical ice bath. In total, 26 sensors were spaced between 0.25 and 0.40 m apart, along 7 m of the thermistor string. The string was installed in a borehole drilled with pressurised hot water which was then backfilled with fine surface snow. The borehole drilling introduces a minor thermal disturbance to the firn, and so data from the first 5 days were discarded as a precaution.

Appendix E: Radar Scatterometry

Radar scatterometry is an active remote sensing technique that is sensitive to the presence of liquid water in snow or firn. To estimate the number of melt days for each winter, we use SeaWinds QuikSCAT Ku-band (2000–2009) and ASCAT C-band (2010–2016) enhanced resolution (4.45 km effective) backscatter products (ftp://ftp.scp.byu.edu/pub/). To maximize consistency in melt detection between the two sensors, we chose the morning overpass, vertical-polarization QuikSCAT product and the "all-pass" ASCAT product, also vertically polarized. This may underestimate the number of melt days for the QuikSCAT era, as more overpasses are available per day. A melt day was recorded if backscatter dropped more than a chosen threshold below the mean backscatter of the previous winter season. For QuikSCAT, the threshold was 3 dB (Luckman et al., 2014; Trusel et al., 2012). A lower threshold of 2.7 dB was chosen for ASCAT due to the reduced sensitivity of C-band microwaves.

Acknowledgments
We would like to thank the British Antarctic Survey logistics team. Funding of this research was through the Netherlands Earth System Science Centre (NESSC), the Netherlands Organization for Scientific Research (NWO), and NERC grant NE/L006707. E. G. and A. O. acknowledge use of the MONSooN system, supplied by the Joint Weather and Climate Research Programme (Met Office and NERC). The SAR data used in this study are modified Copernicus Sentinel data (2016), processed by the European Space Agency (ESA). All observational data are available at the NERC Polar Data Centre: http://doi.org/10.5285/e3616d28-759e-4cca-8fae-fe398f9552ba, and http://doi.org/10.5285/05c9124b-7119-4d99-8e17-ab754eb3f51c. The authors declare no conflict of interest.

References

Abram, N. J., Mulvaney, R., Wolff, E. W., Triest, J., Kipfstuhl, S., Trusel, L. D., et al. (2013). Acceleration of snow melt in an Antarctic Peninsula ice core during the twentieth century. *Nature Geoscience*, *6*, 404–411. https://doi.org/10.1038/ngeo1787

Banwell, A. F., MacAyeal, D. R., & Sergienko, O. V. (2013). Breakup of the Larsen B Ice Shelf triggered by chain reaction drainage of supraglacial lakes. *Geophysical Research Letters*, *40*, 5872–5876. https: //doi.org/10.1002/2013GL057694

Bassis, J. N., & Walker, C. C. (2012). Upper and lower limits on the stability of calving glaciers from the yield strength envelope of ice. *Proceedings of the Royal Society*, *468*, 913–931. https://doi.org/10.1098/rspa.2011.0422

Bell, R. E., Chu, W., Kingslake, J., Das, I., Tedesco, M., Tinto, K. J., et al. (2017). Antarctic ice shelf potentially stabilized by export of meltwater in surface river. *Nature*, *544*, 344–348. https://doi.org/10.1038/nature22048

Cape, M. R., Vernet, M., Skvarca, P., Marinsek, S., Scambos, T., & Domack, E. (2015). Foehn winds link climate-driven warming to ice shelf evolution in Antarctica. *Journal of Geophysical Research: Atmospheres*, *120*, 11,037–11,057. https://doi.org/10.1002/2015JD023465

De Angelis, H., & Skvarça, P. (2003). Glacier surge after ice shelf collapse. *Science*, *299*, 1560–1562.

DeConto, R. M., & Pollard, D. (2016). Contribution of Antarctic to past and future sea-level rise. *Nature*, *531*, 591–597. https://doi.org/10.1038/nature17145

Depoorter, M. A., Bamber, J. L., Griggs, J. A., Lenaerts, J. T. M., Ligtenberg, S. R. M., van den Broeke, M. R., & Moholdt, G. (2013). Calving fluxes and basal melt rates of Antarctic ice shelves. *Nature*, *502*, 89–92. https://doi.org/10.1038/nature12567

Elvidge, A. D., & Renfrew, I. A. (2016). The causes of foehn warming in the lee of mountains. *Bulletin of the American Meteorological Society*, *97*(3), 455–466.

Elvidge, A. D., Renfrew, I. A., King, J. C., Orr, A., Lachlan-Cope, T. A., Weeks, M., & Gray, S. L. (2014). Föhn jets over the Larsen C Ice Shelf, Antarctica. *Quarterly Journal of the Royal Meteorological Society*, *141*, 698–713. https://doi.org/10.1002/qj.2382

Gladish, C. V., Holland, D. M., Holland, P. R., & Price, S. F. (2012). Ice shelf basal channels in a coupled ice-ocean model. *Journal of Glaciology*, *58*(252), 1227–1244. https://doi.org/10.3189/2012JoG12J003

Harig, C., & Simons, F. J. (2015). Accelerated West Antarctic ice mass loss continues to outpace East Antarctic gains. *Earth Planet Science Letters*, *415*, 134–141. https://doi.org/10.1016/j.epsl.2015.01.029

Hubbard, B., Luckman, A., Ashmore, D., Bevan, S., Kulessa, B., Kuipers Munneke, P., et al. (2016). Massive subsurface ice formed by refreezing of ice-shelf melt ponds. *Nature Communications*, *7*, 11897. https://doi.org/10.1038/ncomms11897

King, J. C., Kirchgaessner, A., Bevan, S., Elvidge, A. D., Kuipers Munneke, P., Luck, A., et al. (2017). The impact of föhn winds on surface energy balance during the 2010–2011 melt season over Larsen C Ice Shelf, Antarctica. *Journal of Geophysical Research: Atmospheres*, *122*, 12,062–12,076. https://doi.org/10.1002/2017JD026809

Kingslake, J., Ely, J. C., Das, I., & Bell, R. (2017). Widespread movement of meltwater onto and across Antarctic ice shelves. *Nature*, *544*, 349–352. https://doi.org/10.1038/nature22049

Kuipers Munneke, P., Ligtenberg, S. R. M., van den Broeke, M. R., van Angelen, J. H., & Forster, R. R. (2014). Explaining the presence of perennial liquid water bodies in the firn of the Greenland Ice Sheet. *Geophysical Research Letters*, *41*, 476–483. https://doi.org/10.1002/2013GL058389

Kuipers Munneke, P., Picard, G., van den Broeke, M. R., Lenaerts, J. T. M., & Meijgaard, E. (2012). Insignificant change in Antarctic snowmelt volume since 1979. *Geophysical Research Letters*, *39*, L01501. https://doi.org/10.1029/2011GL050207

Kuipers Munneke, P., van den Broeke, M. R., King, J. C., Gray, T., & Reijmer, C. H. (2012). Near-surface climate and surface energy budget of Larsen C ice shelf, Antarctic Peninsula. *The Cryosphere*, *6*, 353–363. https://doi.org/10.5194/tc-6-353-2012

Leeson, A. A., van Wessem, J. M., Ligtenberg, S. R. M., Shepherd, A., van den Broeke, M. R., Killick, R., et al. (2017). Regional climate of the Larsen B embayment 1980–2014. *Journal of Glaciology*, *63*(240), 683–690. https://doi.org/10.1017/jog.2017.39

Lenaerts, J. T. M., Lhermitte, S., Drews, R., Ligtenberg, S. R. M., Berger, S., Helm, V., et al. (2016). Meltwater produced by wind-albedo interaction stored in an East Antarctic ice shelf. *Nature Climate Change*, *7*, 58–62. https://doi.org/10.1038/nclimate3180

Luckman, A., Elvidge, A., Jansen, D., Kulessa, B., Kuipers Munneke, P., King, J., & Barrand, N. E. (2014). Surface melt and ponding on Larsen C Ice Shelf and the impact of föhn winds. *Antarctic Science*, *26*(6), 625–635. https://doi.org/10.1017/S0954102014000339

Marshall, G. J. (2003). Trends in the Southern Hemisphere Annular Mode from observations and reanalyses. *Journal of Climate*, *16*, 4134–4143.

Marshall, G. J., Orr, A., van Lipzig, N., & King, J. C. (2006). The impact of a changing Southern Hemisphere Annular Mode on Antarctic Peninsula summer temperatures. *Journal of Climate*, *19*, 5399–5405. https://doi.org/10.1175/Jcli3844.1

Orr, A., Marshall, G. J., Hunt, J. C. R., Sommeria, J., Wang, C.-G., van Lipzig, N. P. M., et al. (2008). Characteristics of summer airflow over the Antarctic Peninsula in response to recent strengthening of westerly circumpolar winds. *Journal of the Atmospheric Sciences*, *65*, 1396–1413. https://doi.org/10.1175/2007JAS2498.1

Orr, A., Phillips, T., Webster, S., Elvidge, A., Weeks, M., Hosking, S., & Turner, J. (2014). Met Office Unified Model high-resolution simulations of a strong wind event in Antarctica. *Quarterly Journal of the Royal Meteorological Society*, *140*(684), 2287–2297.

Phillips, T., Rajaram, H., & Steffen, K. (2010). Cryo-hydrologic warming: A potential mechanism for rapid thermal response of ice sheets. *Geophysical Research Letters*, *37*, L20503. https://doi.org/10.1029/2010GL044397

Rott, H., Müller, F., Nagler, T., & Floricioiu, D. (2011). The imbalance of glaciers after disintegration of Larsen-B ice shelf, Antarctic Peninsula. *The Cryosphere*, *5*, 125–134. https://doi.org/10.5194/tc-5-125-2011

Scambos, T. A., Hulbe, C., Fahnestock, M., & Bohlander, J. (2000). The link between climate warming and break-up of ice shelves in the Antarctic Peninsula. *Journal of Glaciology*, *46*, 516–530.

Sergienko, O. V. (2013). Basal channels on ice shelves. *Journal of Geophysical Research: Earth Surface*, *118*, 1342–1355. https://doi.org/10.1002/jgrf.20105

Simpkins, G. R., & Karpechko, A. Y. (2012). Sensitivity of the Southern Annular Mode to greenhouse gas emission scenarios. *Climate Dynamics*, *38*, 563–572. https://doi.org/10.1007/s00382-011-1121-2

Steinhart, J. S., & Hart, S. R. (1968). Calibration curves for thermistors. *Deep Sea Research and Oceanographic Abstracts*, *15*, 497–503.

Trusel, L. D., Frey, K. E., & Das, S. B. (2012). Antarctic surface melting dynamics: Enhanced perspectives from radar scatterometer data. *Journal of Geophysical Research*, *117*, F02023. https://doi.org/10.1029/2011JF002126

Trusel, L. D., Frey, K. E., Das, S. B., Kuipers Munneke, P., & van den Broeke, M. R. (2013). Satellite-based estimates of Antarctic surface meltwater fluxes. *Geophysical Research Letters*, *40*, 6148–6153. https: //doi.org/10.1002/2013GL058138

Van den Broeke, M. R., König-Langlo, G., Picard, G., Kuipers Munneke, P., & Lenaerts, J. (2010). Surface energy balance, melt and sublimation at Neumayer station (East Antarctica). *Antarctic Science*, *22*(1), 87–96. https://doi.org/10.1017/S0954102009990538

Van den Broeke, M. R., Reijmer, C. H., van As, D., van de Wal, R. S. W., & Oerlemans, J. (2005). Seasonal cycles of Antarctic surface energy balance from automatic weather stations. *Annals of Glaciology*, *41*, 131–139.

Van Wessem, J. M., van de Berg, W. J., Noël, B. P. Y., van Meijgaard, E., Birnbaum, G., Jakobs, C. L., et al. (2017). Modelling the climate and surface mass balance of polar ice sheets using RACMO2, part 2: Antarctica (1979–2016). *The Cryosphere*, *12*, 1479–1498. https://doi.org/10.5194/tc-12-1479-2018

Wang, W., Zender, C. S., van As, D., Smeets, C. J. P. P., & van den Broeke, M. R. (2016). A Retrospective, Iterative, Geometry-Based (RIGB) tilt-correction method for radiation observed by automatic weather stations on snow-covered surfaces: Application to Greenland. *The Cryosphere*, *10*, 727–741. https://doi.org/10.5194/tc-10-727-2016

Zheng, F., Li, J., Clark, R. T., & Nnamchi, H. C. (2013). Simulation and projection of the Southern Hemisphere Annular Mode in CMIP5 models. *Journal of Climate*, *26*, 9860–9879. https://doi.org/10.1175/JCLI-D-13-00204.1